We are IntechOpen,
the world's leading publisher of
Open Access books
Built by scientists, for scientists

5,800
Open access books available

142,000
International authors and editors

180M
Downloads

Our authors are among the

154
Countries delivered to

TOP 1%
most cited scientists

12.2%
Contributors from top 500 universities

CLARIVATE ANALYTICS
BOOK CITATION INDEX
INDEXED

WEB OF SCIENCE™

Selection of our books indexed in the Book Citation Index
in Web of Science™ Core Collection (BKCI)

Interested in publishing with us?
Contact book.department@intechopen.com

Numbers displayed above are based on latest data collected.
For more information visit www.intechopen.com

Chapter

Coconut Shell Charcoal Adsorption to Remove Methyl Orange in Aqueous Solutions

Isabel Cristina Páez-Pumar Romer,
Isabella Victoria Plazola Santana,
Rosa María Rodríguez Bengoechea
and Miguel Manuel Pérez Hernández

Abstract

Activated charcoal was prepared and characterized from residues of coconut peel (CACC) to remove by adsorption the Methyl Orange (AM) dye in aqueous solution. The charcoal was activated with phosphoric acid. The morphology and structure of the pores of the carbon obtained were analyzed by Scanning Electron Microscopy (SEM) and a surface analyzer. The adsorption data were evaluated by the BET, Langmuir and Freundlich isotherms, finding the Langmuir type I model. The surface area of the activated carbon was 526 m^2/g with a pore volume of 0.234 cm^3/g and an average pore diameter of 1.78 nm, according to BET, which indicates the presence of micropores. The calculated thermodynamic parameters showed that the adsorption of the AM dye in CACC is a spontaneous process at room temperature and that physisorption and chemisorption are probably involved. The adsorption tests were followed by UV–visible spectrophotometry. The effects of the adsorbate concentration (AM) and the heat treatment (450–500°C) with an air atmosphere were investigated, keeping constant the stirring time and the H_3PO_4/sample weight ratio. The results obtained indicate that the activated carbon obtained could be used as an alternative low-cost adsorbent in the removal of AM from effluents in aqueous solution.

Keywords: waste, colorant, Langmuir, spontaneous, chemisorption, spectrophotometer

1. Introduction

With economic and technological development, water pollution is a common problem around the world, particularly in the textile, printing paper, pharmaceutical, food manufacturing industry, and in research laboratories [1–3]. Activated charcoal

(AC) shows great capacity as adsorbent in water purification or industrial effluent treatment due to its high pore volume, large specific surface area, high degree of surface reactivity, and effective adsorption quality [4–6]. This adsorption method allows the removal of up to 90% of pollutants; however, the process efficiency will depend on the physicochemical properties of the adsorbent and adsorbate [7]. Additionally, the high-cost and commercially available nonrenewable source of AC limits its use as an adsorbent in developing countries [8]. In recent years, the production of AC from cheap and renewable precursors (recyclable material), such as walnut shells, fruit seeds, pineapple, bagasse, bamboo, rice husk, cotton stems, eggshell, has been studied [9–12]. Coconut shell is a potential precursor for AC production due to its excellent natural structure and low ash content.

Converting coconut shells to activated charcoal would add value to these agricultural products, help reduce the cost of waste disposal, and provide a potentially inexpensive alternative to existing commercial charcoals [13]. The charcoal obtained from this recycling material could function as a good colorant remover in the water purification process, through adsorption processes, as proposed in this work. It is chosen to work with methyl orange (MO) as adsorbent because it is one of the anionic dyes most used in textile industries, [14, 15]; thus, for the purposes of this research, it is considered representative. The adsorption process consists mainly of two stages: first, the passage of the adsorbate through the porous network (diffusion) and the second, the interactions between the adsorbate and the adsorbent. This last step constitutes an important factor considering that some pharmaceutical compounds and organic dyes have diffusive limitations due to their large molecular size [16, 17].

For the preparation of activated charcoal, there are two methods that are mainly used: physical activation (heat treatment, at temperatures that can vary between 400 and 650°C) and chemical activation. In chemical activation, prior heat treatment, the precursor is reacted with an activating chemical agent. Acids, alkalis, and salts in solid state or solution are often used as chemical activating agents. These activating agents promote dehydration and then structural rearrangement at relatively low temperatures [18, 19].

Although porosity is the main characteristic related to the adsorption capacity of activated charcoal (this property will not be determined from a quantitative point of view in this work), the surface chemical composition also plays an important role in said adsorption when specific physical and/or chemical interactions are considered because it determines the moisture content, the catalytic properties, their acidic or basic character, and adsorption of polar species [20, 21].

The main objective of this research is to synthesize and evaluate the charcoal adsorptive capacity that is obtained from the recycling material and verify its adsorption capacity through the removal of methyl orange dye (MO) in aqueous solutions. The operation effects such as the initial concentration of MO were studied, a single type of activating agent was maintained (phosphoric acid), the same average particle size of charcoal was used, the temperature and activation time were a constant [19], the same charcoal/activator ratio and the same initial pH were preserved.

2. Material and methods

2.1 Raw material treatment

The coconut, *Cocos nucifera L.*, is a perennial tropical crop, which involves more than 4000 agricultural producers in Venezuela, and in recent years, the coconut

production has ranged between 130,000 and 178,000 tons [22]. From the coconut that is formed by the shell or husk (endocarp), water, or copra (flesh), the endocarp represents about 30% weight [22].

The coconut shells constitute a recycling material, which are collected from different places located in Chacao municipality, Caracas, Venezuela. Initially, these shells were subjected to a conditioning process, in order to remove the pulp remains that were adhered to the shell and separate the endocarp from the rest of the coconut. Afterward, they were crushed to reduce their size to smaller particles suitable for sample carbonization. Later, they were sieved up to a size of 2–4 mm to obtain uniform samples. Finally, they were stored in a desiccator.

2.2 Preparation and chemical activation of charcoal samples

The samples were prepared by a chemical activation in two steps. In the first step, after the coconut shells were sieved, they were carbonized in a ceramic crucible in air atmosphere, at atmospheric pressure, up to temperatures of 450°C and 500°C (heat treatment), respectively. According to previous research [23], initially, the samples were placed in the horizontal muffle (brand Felisa FE-340) at 300°C. Fifteen minutes later, the temperature was increased to 50°C/15 minutes, and they were kept for 1 hour at the chosen temperatures. Then, the carbonized samples were crushed and sieved again, in order to achieve particle sizes between 150 and 250 μm. In the second step, after carbonization (heat treatment), the samples were impregnated with a solution that was prepared with distilled water at 80% v/v de H_3PO_4 (reagent grade ≥ 85% weight, Honeywell Riedel-de Haën AG), in a precipitation flask, in the ratio 1:2, g charcoal/m phosphoric acid. Then, the samples were dried in an oven at 105°C for a period of 12 hours [24]. Afterward, the sample was activated, which was introduced into the same muffle at a heating rate of 5°C/ up to the final temperature of 600°C in air atmosphere, for a period of 2 hours. The product was cooled to room temperature and washed according to the methodology described by De la Hoz, et al. [25], to remove the phosphoric acid residues that are present in it. The washing was carried out with distilled water at a 0.1 M up to pH 7. To conclude, the samples were dried in the oven at 100°C for 24 hours to remove traces of water from the charcoal.

2.3 Studied adsorbate

Methyl Orange (MO), also called Helianthine or Acid Orange 52, is an anodic dye, which is soluble in water and is used in the textile industry as an acid–base indicator. Its commercial compound name is 4-dimethylaminoazobenzene sulfonic acid sodium salt. Its molecular formula is $C_{14}H_{14}N_3NaO_3S$, and its molecular weight is 327.34 g/mol. **Figure 1**.
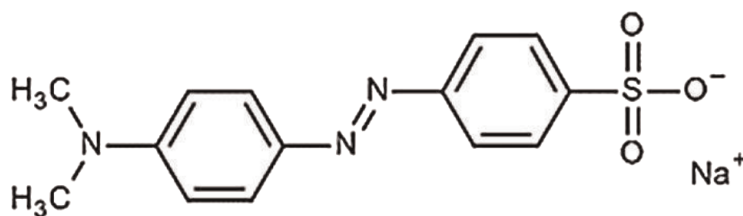
Figure 1.
Developed structure of OM, source: Academic (2010) [26].

The MO is in a solid state as a yellow or orange powder or crystals, it has not odor and is soluble in water. As MO is composed of aromatic rings, it is carried out by interactions between the π bonds of the aromatic ring and those that are found in the charcoal surface [27]. In the basic form of MO, the hydrogen ion is lost from the bridge –N=N- between the rings, and the electrons used to bind the hydrogen neutralize the positive charge on the terminal nitrogen, so that it is no longer able to form the bond π [28] (**Figure 2**). The color of MO solutions is yellow in alkaline medium.
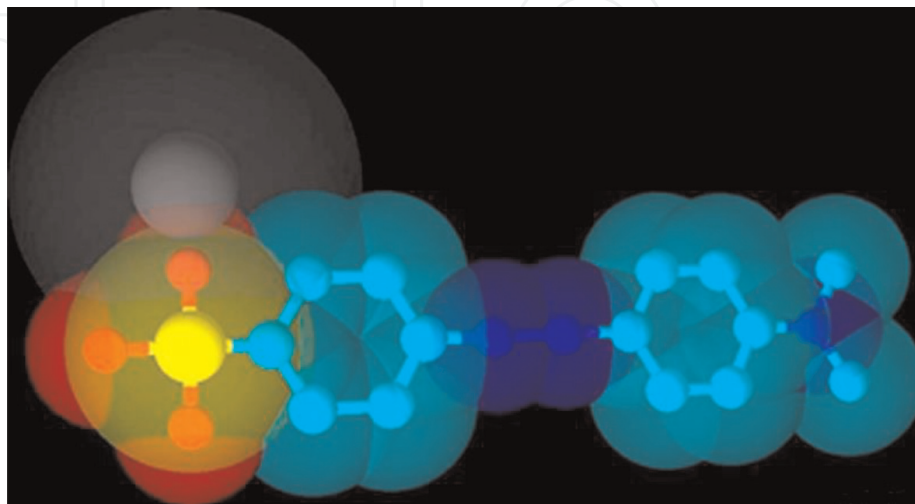
Figure 2.
*View of the methyl orange molecule with the presence of Van der Waals forces. **[HHH]**, edited with ACD/3D viewer 2019.2.0 (file version D05E41, build 108,653, Apr 25, 2019).*

This azo-derived chemical compound with weak acid characteristics presents health risks in an aqueous medium, which is why several water treatments are practiced for its removal, such as degradation under irradiation or electrocoagulation [29].

D. A. Kron et al. demonstrated that Methyl Red (sodium salt) has dimensions of 1.61 nm length and 0.88 nm width [30]. Because the MO has a similar structure to methyl red, it is reasonable to expect that MO dimensions to be similar to methyl red. Methyl Orange (MO) is one of the most widely used anionic dyes in these industries, the presence of azo group (-N=N-) in its molecule, its low biodegradability, and its high solubility in water make it a serious threat for the environment [14, 15].

3. Synthetic solution preparation of methyl orange dye

Residual aqueous solutions of dye were simulated with different concentrations of MO (400, 200, 80 y 40 mg/L) [31]. The solutions were prepared with distilled water and analytical reagent grade MO (Merck).

3.1 Characterization of coconut shell charcoal

The porous structure of the coconut shell charcoal obtained was characterized by the nitrogen adsorption–desorption technique using the automatic instrument TriStar ® 3000 V2.0 from Micromeritics I. Corp., USA., at liquid nitrogen temperature (77 K). The specific surface area (SBET) of activated charcoal was calculated by using the Brunauer–Emmett–Teller (BET) equation, assuming that the area of nitrogen molecule is 0.162 nm^2. The total pore volume was estimated as the liquid volume of adsorbate adsorbed (N_2), at a relative pressure (P/Po) of 0.99 (**Table 1**).

Area	
BET surface area	526.47 m^2/g
Micropore area, t-Plot	463.75 m^2/g
External surface area, t-Plot	62.72 m^2/g
Volume	
Total pore Volume (a)	0.2341 cm^3/g
Adsorbed volume	120.94 cm^3/g STP
Micropore volume, t-Plot.	0.1762 cm^3/g
Mesopore volume, BJH (b)	0.03641 cm^3/g
Pore Volume	
Average pore diameter (4 V/A, BET)	1.7784 nm
Average pore diameter (4 V/A, BJH)	7.7859 nm

Source: Materials characterization laboratory report, INTEVEP.

Table 1.
Texture properties that were obtained through the adsorption/desorption studies of N$_2$. Parameters of the charcoal obtained. (a) Adsorption, total pore volume of less than 212.7 nm in diameter of the charcoal obtained at P/Po 0.99; (b) adsorption, cumulative pore volume of pores between 1.7 and 300 in diameter.

The micropore volume and the microporous surface area were determined by the t-Plot method [32]. The external surface area (which is the surface covered by mesopores and macropores) was calculated by the difference of the BET surface area, and the microporous surface was calculated from the t-Plot graph. The t-Plot method that was designed by De Boer et al. and Sing and referenced by Coasne et al. [33], is a well-known technique that allows determining the micro- and/or mesoporous volumes and the specific surface area of a sample, in comparison with a reference adsorption isotherm of a nonporous material that has the same surface chemistry. In order to observe the morphology of the activated charcoal that is obtained from the coconut shell, Scanning Electron Microscopy was used. For the sample preparation, the cathodic sputtering technique was used. The process was carried out under a pressure of 0.1 mbar and 20 mA for 20 minutes. (Scanning Electron Microscope, Brand JEOL®, Model JSM-6390).

4. Adsorption studies

The adsorption experiments were conducted in batch or discontinuous mode, mixing 25 mL of a dye solution of known concentration of 0.1 of charcoal, using the charcoals prepared at 450°C and 500°C [34]. The effect of the initial concentration of MO (400 and 200 mg/L), contact time (2 hours) [34], and temperature (25°C) was studied on the MO adsorption with stirring speed of 200 rpm and initial pH indicated in **Table 2**.

It is known that the pH of the solution is important in the adsorption of MO on Activated Charcoal [35–37]. The highest adsorption capacity is obtained toward acid pH, between pH 3 and pH 5. Different authors attribute this effect to the variation in the properties of the adsorbent surface and also to the ionization degree [38].

pH	5.87	5.85	5.77	5.76
C(MO), mg/L	40	80	200	400

Table 2.
Initial pH value for different MO concentrations, in mg/L.

After the adsorption, the samples were filtered by gravity in a precipitation flask to obtain a charcoal-free solution. The resulting liquid was centrifuged for 15 minutes at a stirring speed of 2400 rpm using a tabletop centrifuge (Gemmy Industrial Corp. ® Modelo PLC-05, Taiwan), in order to separate the residual charcoal particles. Finally, the supernatant that was contained in the centrifuge tube was sucked out. The supernatant was analyzed by a calorimeter method using a UV–visible spectrophotometer, brand Fisher ® 4001/4, Thermo Scientific, Genesys 20, U.S.A, at a wavelength of 520 nm [39–41].

MO concentrations in aqueous solution were determined by using the data of the calibration curve, concentration based on absorbance, by means of Eq. (1):

$$C = k.Abs + b \tag{1}$$

Where C is the concentration of methyl orange, mg/L, Abs is the absorbance, and k, b are the constants for the adjustment. Since the spectrophotometer was calibrated with distilled water, the b term is equal to zero. The MO concentration was established by measuring the absorbance and substituting it in the equation of the calibration curve. With the calibration curve obtained and the absorbance indicated by the equipment, the final concentration of solution was calculated, and later, based on the results obtained, the optimum carbonization temperature was determined. The tests were carried out in triplicate.

The MO adsorption capacity at equilibrium, qe (mg/g), and the removal efficiency Q (%) were obtained according to the Eqs. (2) and (3), respectively:

$$qe = \frac{(Co - Cf).V}{W} \tag{2}$$

$$Q = \frac{(Co - Cf).100}{Co} \tag{3}$$

Where V(L) is the solution volume, W(g) is the adsorbent amount, C_0 (mg/L) is the initial concentration of MO, and Cf (mg/L) is the MO concentration at equilibrium.

4.1 Adsorption isotherm studies

Adsorption isotherms provide information regarding the adsorbent capacity and the nature of the sorbent-solute interaction. Additionally, the isotherm constant values are essential to predict the maximum adsorption capacity, describing the affinity and the adsorbent surface properties. To describe the adsorption process of MO on activated charcoal that was obtained from the coconut shell, three traditional adsorption isotherms are used at 298 K: the Langmuir model [42], Freundlich model [43], and Brunauer–Emmett–Teller (BET) model [44].

4.2 Langmuir isotherm

The Langmuir Adsorption Isotherm is obtained once the adsorption is restricted by the formation of the monolayer when the adsorbate covers the adsorbent, it covers the monolayer and the process stops [45]. It is based on the hypothesis that states "all active adsorption centers are equivalent and the ability of a molecule to bind to the surface is independent whether or not there are nearby positions occupied" [46].

The linear representation of the Langmuir isotherm is represented by the Eq. (4):

$$\frac{C_e}{q_e} = \frac{1}{q_m K_L} + \frac{C_e}{q_m} \tag{4}$$

Where: q_m represents the maximum absorbent amount of monolayer (mg/g), K_L is the constant of Langmuir adsorption (L/mg) and is related to the free energy adsorption and temperature function. C_e is the concentration of the solution at equilibrium; q_e is the amount of adsorbate adsorbed at equilibrium per unit mass of the adsorbent (mg/g).

The essential characteristics of Langmuir isotherm can be expressed in terms of the equilibrium or separation parameter, called R_L factor, which is a dimensionless constant, Eq. (5) [47, 48]:

$$R_L = \frac{1}{1 + K_L C_o} \tag{5}$$

The R_L value indicates that the nature of adsorption is unfavorable ($R_L > 1$), linear ($R_L = 1$), favorable ($0 < R_L < 1$), or irreversible ($R_L = 0$). On the other hand, depending on the type of associated isotherm to Langmuir, the porosity characteristics associated with the material can be inferred [49].

4.3 Freundlich isotherm

The Freundlich adsorption isotherm model is an empirical equation that expressed the heterogeneity of the adsorbent material and multilayer coverage of adsorbate, its linear equation is represented by the Eq. (6)

$$ln\, q_e = ln\, K_F + \frac{1}{n} ln\, C_e \tag{6}$$

Where K_F is the Freundlich constant (mg/g) and is related to the adsorption capacity (bond strength), n is a parameter that measures the intensity of adsorption bond between the adsorbate and adsorbent.

4.4 Brunauer, Emmett Teller isotherm

The Brunauer, Emmett Teller (BET) isotherm model is an extension of the Langmuir model to the multilayer adsorption. It is not limited to the formation of monolayer, but the adsorption process is carried out until adsorbent surface is fully covered by a multimolecular or multilayer, which can be applied to both flat and convex surfaces [45]. The BET isotherm considers more real conditions and works under fewer assumptions, unlike Langmuir, which is why it is more successful to handle BET isotherm when it is required to reduce the surface area.

Its linearized form that allows direct graphic representation from the experimental data of the adsorption isotherm is presented in Eq. 7.

$$\frac{P}{V(Po - P)} = \frac{1}{V_m K} + \frac{K - 1}{V_m K} + \frac{P}{Po} \tag{7}$$

Where P is the pressure after the adsorption process; Po, the liquefaction of gas pressure; V is the volume adsorbed per gram of adsorbent; Vm, is the volume associated with the monolayer formation; K is a constant that depends on the temperature but does not depend on the surface coating [49].

To calculate the adsorbent surface area, the following equation was used:

$$A = \frac{V_m}{22400} N.\sigma.10^{-20} \tag{8}$$

Where: A is the adsorbent surface area (m^2/g), Vm is expressed in cm^3/g adsorbent, 22,400 is the molar volume in STP, N = Avogadro's Number, σ = adsorbate molecular area, in this case N_2 normally in Amgstrom^2 [45].

4.5 Thermodynamics of adsorption

The results of thermodynamic studies are useful to understand the viability of the adsorption process to obtain useful information regarding fundamental thermodynamic parameters of adsorption that are, such as the standard free energy change (ΔG^o). If the adsorption isotherms that were experimentally obtained are adequately described by the Langmuir's equation, then the thermodynamic parameters can be calculated by the Eqs. (9) and (10):

$$K = K_L.\gamma \tag{9}$$

$$\Delta G^o = -RTlnK \tag{10}$$

Where K is the dimensionless constant, K_L is the adsorption constant expressed in L/mol, γ is the amount of solvent in 1 kg of its weight (for water γ = 55.5 mol/L, water density 1 kg/L) [50, 51], R is the universal gas constant (8.31434 J/mol.K), and T is the absolute temperature.

5. Results and discussion

5.1 Optimal carbonization temperature

The charcoal obtained from the first carbonization at 450°C and 500°C, without being chemically activated, was subjected to adsorption tests with methyl orange solutions (200 mg/L and 400 mg/L), in order to determine which of these samples adsorbed more colorant. **Figure 3** shows that there is a higher percentage of MO adsorbed at 450°C rather than at 500°C. This difference in adsorption percentages between the charcoal obtained at 450°C and 500°C may be because the latter has a higher percentage of ash, which can interfere with the adsorption of the colorant, considering that these ashes are impurities that harm the adsorption process.
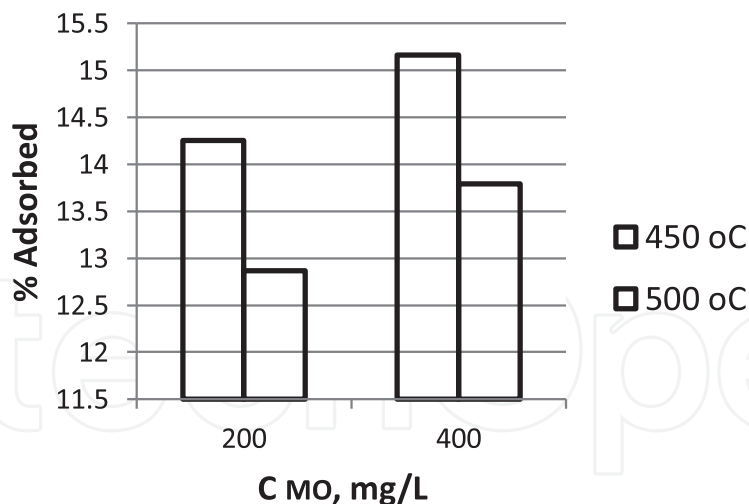
Figure 3.
Comparison of carbonization temperatures (heat treatment,) through methyl orange adsorption, C (MO concentration) at 450°C and 500°C.

5.2 Screening

Particles in the range of 150–250 μm [52] were selected for activation while using a standard analytical screen of frame and mesh. It was decided to sieve the particles obtained, in order to get a more homogeneous charcoal and that the difference in size between particles would not interfere with the adsorption process [34].

5.3 Comparison of charcoal obtained before and after activation

Activated charcoal with heat and chemical treatment showed a higher adsorption capacity with MO when compared with charcoal before the chemical activation process (only with heat treatment.) For the MO solutions of 200 and 400 mg/L, the adsorption increase was 140.6% and 51.3%, respectively, which indicates the effect of chemical activation with phosphoric acid in the adsorption process, see **Table 3**. This can also be compared with the work carried out by Carriazo et al. [53], where similar results are obtained.

It is observed an adsorption percentage increase which is possible because the chemical activation improved the surface area due to increased porosity [54]. Acid (phosphoric acid) impregnation oxidizes the charcoal's porous surface by increasing the hydrophilic locations on the surface [55]. Liquid-phase oxidations especially increase the concentration of carboxylic acids on the charcoal surface [56]. However, this is not evaluated in the present work, since the objective is to establish the adsorptive capacity of a material that is generated from a recycling product, which is why the presence of functional groups is not quantified, but it could be inferred about it, as it is indicated in the investigation carried out by Van Der Kamp et al. [57] and Bernal et al. [58]. By chemically activating the charcoal, the attraction between the adsorbent and the adsorbate increases, new bonds are formed between them, and it can be due to intermolecular forces. This type of initial physical adsorption occurs by weak forces and, generally, nonspecific forces, such as Van der Waals and the London dispersion forces [59–61]. On the other hand, the electrostatic interactions are common in the adsorption of activated charcoal due to the charges that are present when the acids or weak bases are ionized in an aqueous environment. Likewise, the presence of

Co MO (mg/L)	Charcoal (Treatment)	% Adsorbed	Adsorption variation, %
200	Non-activated	14.3	140.6
200	Activated	34.4	
400	Non-activated	15.2	51.3
400	Activated	23	

Table 3.
Comparison of the methyl orange adsorption capacity of the charcoal obtained at 450°C without activating (only with heat treatment) and activated charcoal with phosphoric acid; Co (initial concentration.) variation in the adsorption, percentage.

functional groups on the adsorbent surface generates the formation of dipoles with the adsorbate molecules due to differences in the electronic distributions. Aburub and Wuster [57] mention that specific interactions (ionic interactions, Keeson and Debye forces) are related to adsorption processes, which are directed through enthalpy, while nonspecific interactions (London forces) are related to processes that are carried through entropy [58].

## 5.4 Equilibrium experiments, adsorption isotherms

Adsorption isotherms are the tools used to predict the distribution of adsorbate molecules in the solid–liquid interface when the chemical equilibrium is reached. The MO adsorption isotherms on activated charcoal and the respective adjustments for the Langmuir model were obtained through the data shown in **Table 4** and represented in **Figure 4** where the straight line is reproduced with a coefficient of determination of 0.9822.

The shape of the isotherm adjusts to the Langmuir isotherm type one where a rapid increase in adsorption is observed while the pressure increases and stops when it reaches a limit value. This occurs because in this type of isotherm, the adsorption is restricted by the formation of the monolayer. This type of isotherm is present mostly in chemisorption processes [45]. In **Figure 5**, the monolayer formation is represented where the amount adsorbed increases with the MO concentration until it reaches a limit value, corresponding to the coating of a surface by a monolayer. First, there must be an adsorption–desorption equilibrium process, typical of physical adsorption. Once the monolayer formation is reached, comes the chemisorption process, which is predicted by this isotherm.

| Ce/qe, g/L	qe, mg/g	Co (mg/L)	Ce (mg/L)	Q (%)
0.17	9.59	40	1.65	95.88
1.37	14.91	80	20.38	74.53
7.64	17.19	200	131.25	34.38
13.74	22.54	400	309.83	22.54

Table 4.
MO adsorption on activated charcoal; Co (initial concentration, mg/L), qe (adsorption capacity, mg/g), Q (removal efficiency), V (volume of MO solution, L).

Langmuir Isotherm Equation
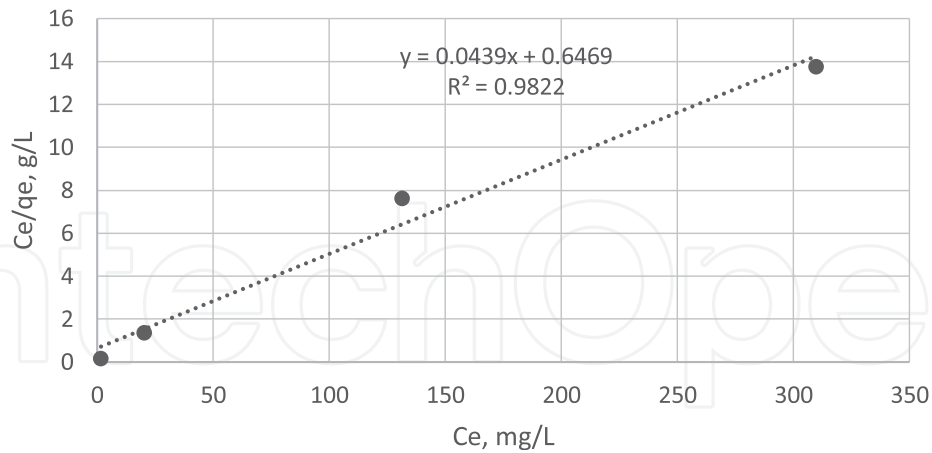
Figure 4.
Equation that represents the Langmuir isotherm, linearized, for the activated charcoal that is obtained from the coconut shell, moles adsorbed per gram of charcoal with respect to the final concentration; Ce: Final concentration of the solution (mg/L); qe: Amount of adsorbate adsorbed in the equilibrium per unit mass of the adsorbent (mg/g).

Langmuir Isotherm
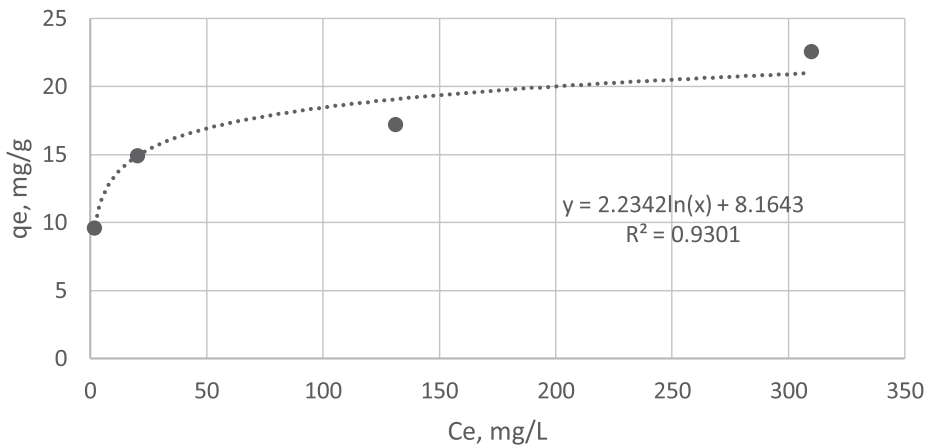
Figure 5.
Langmuir isotherm (type 1.) monolayer formation for activated charcoal from the coconut's endocarp; Ce: Final concentration of the solution; (mg/L) qe: mg adsorbed per gram of adsorbent.

The monolayer formation is reached when the adsorbed mass gets closer to 22.78 mg. A horizontal asymptote is observed when the moles adsorbed per gram of charcoal between the number of adsorption positions that are available in the surface approximate to 1. This type of isotherm is associated with microporous materials [62].

The constant values of the adsorption isotherms are shown in **Table 5**. The applicability of the isotherm equations is compared based on the coefficients of correlation R^2. The coefficient R^2 was lower in Freundlich rather than in Langmuir, which indicates that the MO adsorption in the charcoal activated adsorbent of the coconut shell results from adsorption in the monolayer.

The equilibrium parameter or separation called R_L factor obtained for the different initial concentrations of MO is shown in **Table 6**. The R_L value ($0 < R_L < 1$) indicates that the adsorption nature is favorable.

Langmuir model			Freundlich model		
q_m (mg/g)	K_L (L/mg)	R^2	K_F (mg/g)	n	R^2
22.78	0.0679	0.98225	8.99	0.1514	0.9653

Table 5.
*Parameters of Langmuir and Freundlich isotherms, at 25°C.*

Co (MO) (mg/L)	40	80	200	400
R_L	0.2692	0.1555	0.0686	0.0355

Table 6.
R_L factor (dimensionless) obtained for different initial concentrations of MO (mg/L).

5.5 BET isotherm, pore characteristics, and surface area

The graph obtained for the adsorption–desorption process for the nitrogen on activated charcoal from the coconut endocarp, applying the BET isotherm model, is shown below (**Figure 6**).

On the other hand, the values obtained for the BET isotherm with the activated charcoal were plotted, in order to evaluate its surface area, obtaining the graph shown below. (**Figure 7**).
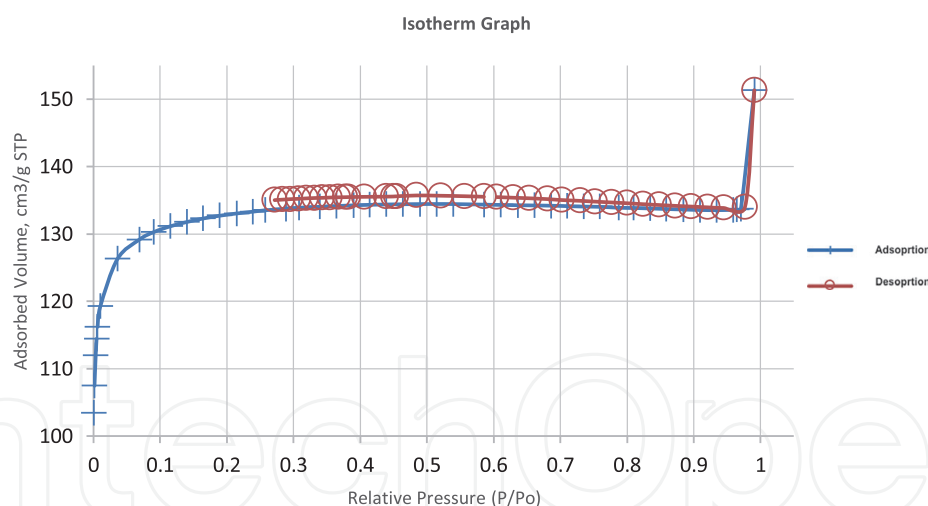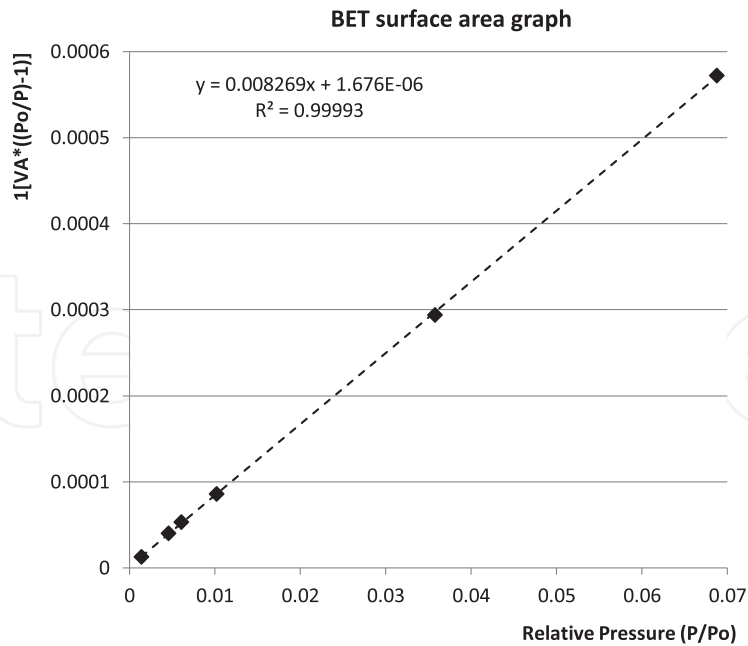

Figure 6.
BET isotherm representation, adsorption–desorption process for activated charcoal from the coconut endocarp; adsorbed volume (cm³/g) STP based on the relative pressure (P/Po.)

The surface area of the activated charcoal was measured by using the Brunauer–Emmett–Teller (BET) model. The surface area according to BET is determined by applying the Eq. (8), and the value obtained of the specific surface area is 526 m²/g. This value coincides with the values reported by [63] similar adsorbents.

Table 1 shows the results obtained for the surface area and pore volume using the BET model.

The total pore volume is estimated from the amount of nitrogen adsorbed at the highest relative pressure and the micropore volume is calculated from the nitrogen adsorption isotherm using the Dubinin-Radushkevich Equation [64].

Figure 7.
BET isotherm representation, linearized, for activated charcoal from the coconut endocarp; 1/[VA*((Po/P)-1)] based on the relative pressure (P/Po).

The method used to determine the distribution of the pore size was the one from BJH [65], which was applied to the nitrogen adsorption data that was measured at 77 K in mesoporous materials. The results obtained match the ones reported by BJH (Barret-Joyner–Halenda), which estimate that the pore volume corresponds to a cylindrical pore volume (**Figure 8**) [65].
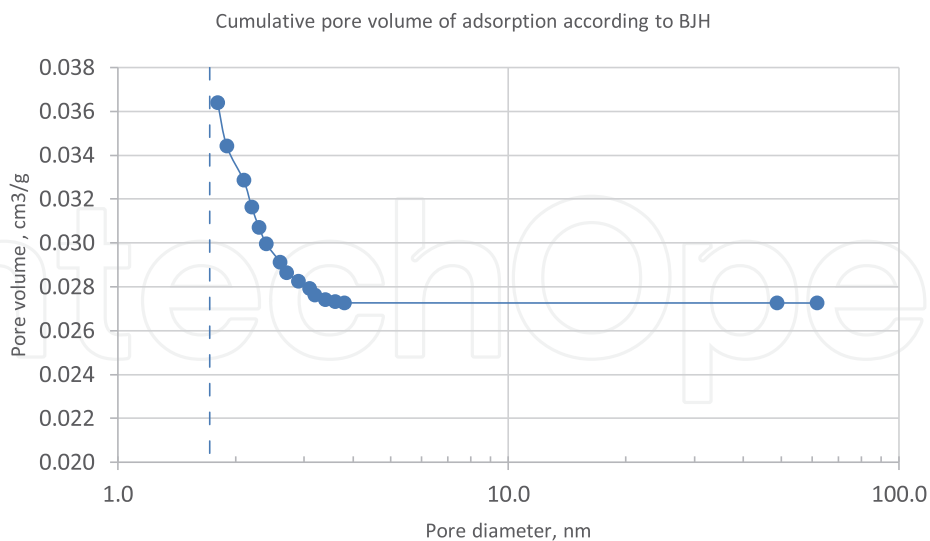
Figure 8.
Representation of pore volume (cm3/g) based on the pore diameter (nm), BJH model.

5.6 Thermodynamics of adsorption

The data that were obtained experimentally from the batch adsorption studies were analyzed using thermodynamic equations expressed before. **Table 7** shows the thermodynamic adsorption values.

K$_L$ (L/mol)	ΔG° (kJ/mol)
22,215	−34.8

Table 7.
Thermodynamic values of MO adsorption on activated charcoal obtained from the coconut endocarp at 25°C.

The negative values of ΔG° at the studied temperature indicate the spontaneity of adsorption process, which reflects the affinity of the charcoal obtained toward the anionic dyes [66, 67]. The determined value is ΔG°$_{ads}$ = −34.8 kJ/mol, which is in the range from −20 kJ/mol to −40 kJ/mol. This probably indicates that physisorption and chemisorption are involved in this process [68]. It was taken into account another author for the calculation of K$_L$ [69], where the ratio of the areas that the solvent and colorant occupy on the surface of the adsorbent is used, the value of ΔG°$_{ads}$ = −30.3 kJ/mol.
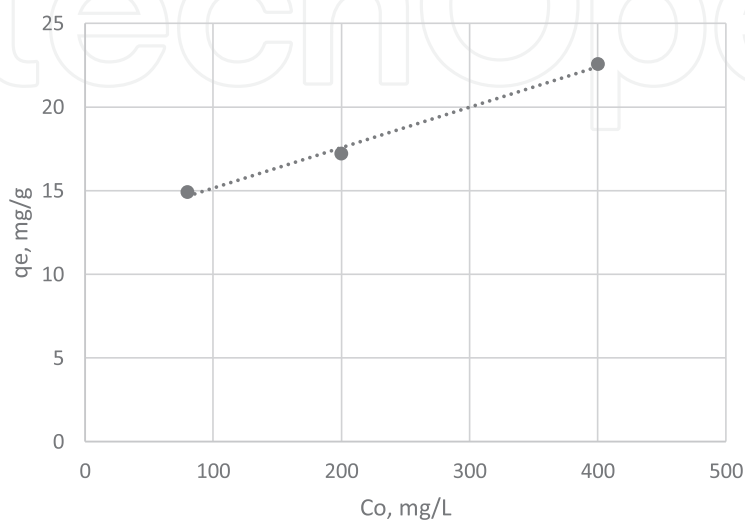
5.7 Effect of MO initial concentration on adsorption

The effect of MO initial concentration on adsorption by activated charcoal is shown in **Figure 9**. It can be seen that the equilibrium adsorption capacity increased almost linearly when the concentration of MO solution increased from 80 to 400 mg/l. This phenomenon can be explained in terms of interactions between the MO anionic molecule and the adsorbent. In this case, the amount of adsorbent is kept constant. When the MO amount per unit volume of solution increases, the ratio of the amount of MO ions in relation to the available adsorption site, at first, also increases and more MO ions in solution can be adsorbed by the activated charcoal. The observed behavior coincides with what was reported by [70].

The dissociation equilibrium of methyl orange is shown in **Figure 1**.

5.8 Morphology. Microstructure evolution of activated charcoal from the coconut shell

From the **Figures 10–12**, the morphology transformation of the coconut endocarp can be visualized. **Figure 10** shows the coconut endocarp without heat treatment.

Figure 9.
*Effect of MO initial concentration on activated charcoal adsorption.*

Figure 11 shows the effect of carbonization on the coconut endocarp, and in **Figure 12**, the activated charcoal can be seen, which is the result from the chemical activation.

In **Figure 10**, the coconut endocarp without heat treatment, at different magnifications, is shown. An irregular morphology composed by fibers, fissures, and cavities is detected, which also indicates the potential of this material to generate activated charcoal, as referred by different authors [71–73]. Katesa et al. [74] concluded in their work that the porous properties of activated charcoal, including the surface area and pore volume, decreased while the carbonization temperature was increased. The lowest carbonization temperature at 250°C produced the activated charcoal with the highest porous properties for the activation temperature at 850° C and 60 and 120 minutes of activation time.

The higher magnification photomicrograph (**Figure 10d**) shows cavities of circular nature.

After carbonization (heat treatment,) an irregular external surface with cracks and non-spherical cavities around 0.1 μm is observed (**Figure 11**). As reported in the literature [71–74], the morphology obtained after heat treatment seems to be a result of the loss of moisture and volatile material that leaves the precursor structure; hence, leaving irregular cavities and transforming the structure of the coconut endocarp.

The activated charcoal shows great porosity where particles from 150 to 250 μm are heterogeneous, as well as their pores have different shapes and sizes, which favor the adsorption process, and it is in these pores where the adsorbate particles are housed, **Figure 12**.
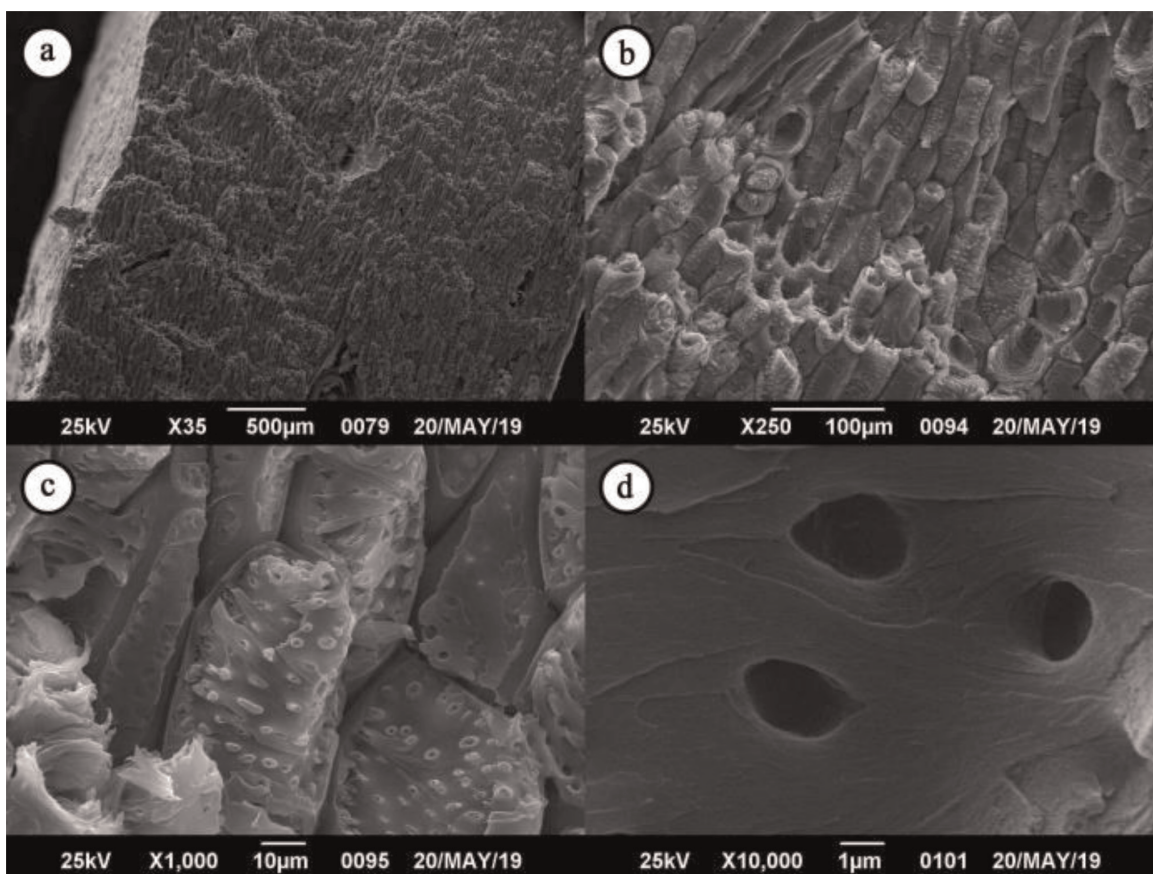
Figure 10.
Coconut endocarp with magnification of: a) 35, b) 250, c) 1000 y d) 10,000 times its size.
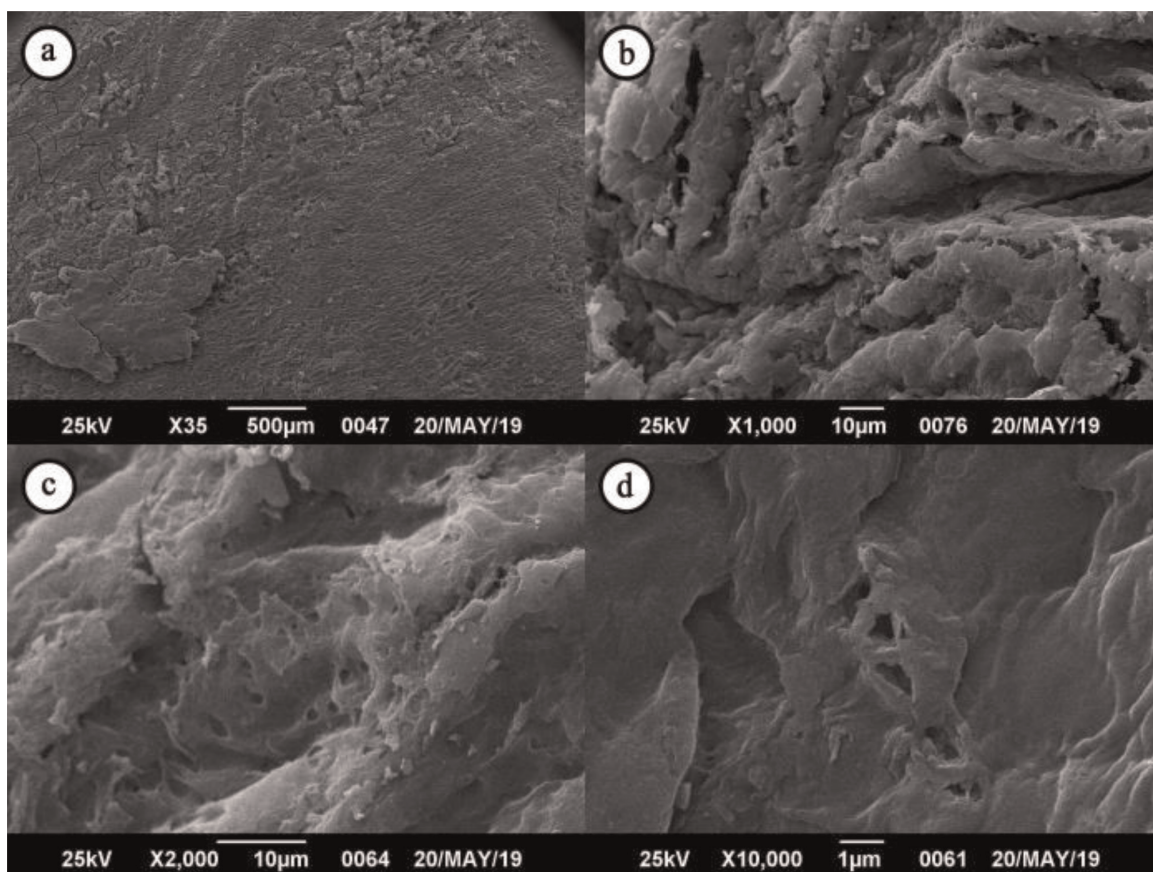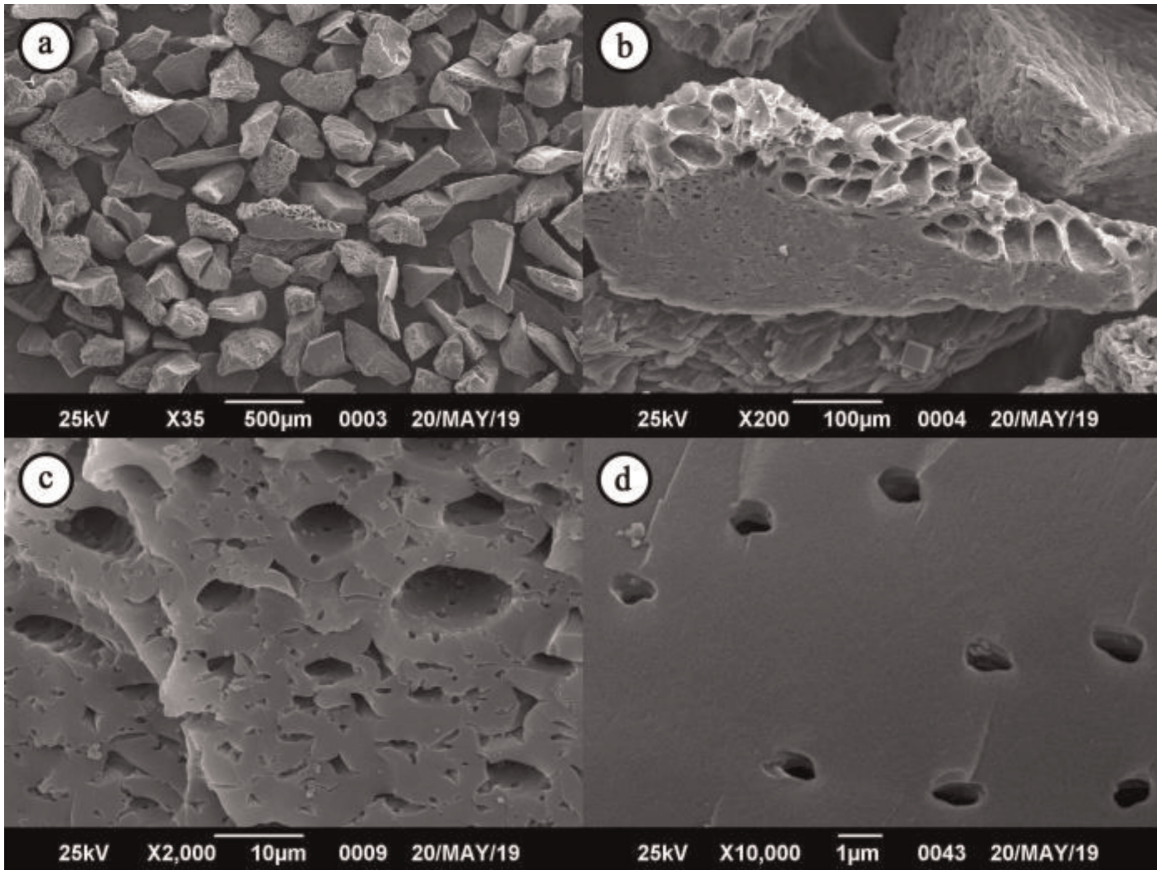
Figure 11.
Carbonized coconut endocarp at different magnifications: a) 35, b) 1000, c) 2000, and d) 10,000 times its size.

Representative images of the activated charcoal sample were selected in which can be observed the diversity in the size of the pore structure. **Figure 12c** shows pores of different sizes, **Figure 12d** shows smaller pore approaching 1000 nm.

Once the material was chemically activated (**Figure 12**), irregular particles, from 150 to 250 μm, and the development of great porosity were observed. This result confirms what is described in the literature [71–73], where it is mentioned that activating agents react with the carbonaceous chain to generate new pores or enlarge existing pores. Another possibility of the development of pores in activated charcoal is the occurrence of thermal stress in the structure of the precursor material that would lead to the formation of different cavities and fissures in the final product. Specifically, in the present study, phosphoric acid was used as an activating agent and expansion of the existing pores in the coconut endocarp was detected, as well as the formation of new macropores, mesopores, and micropores. In **Figure 12c**, macropores of different sizes are seen and in **Figure 12d**, macropores of around 1000 nm can be detailed.

The literature [71, 72] refers to the enormous effort in identifying precise methods and procedures to characterize activated charcoals and, specifically, its pore structure. Indirect techniques make it possible to correlate adsorption measurements with mathematical models and use this information to infer about the porous structure of activated charcoal. In this regard, the BET results of the present study show the presence of micropores with an average pore diameter around 1.7784 nm. On the other hand, the current computerized image analysis allows the conversion from 2D SEM (Scanning Electron Microscopy) to 3D. They open a window to improve the studies of porosity development and characterization of activated charcoal [75, 76], which is out of scope of the present study.

Figure 12.
Activated charcoal from the coconut endocarp with a magnification of: a) 35, b) 200, c) 2000, and d) 10,000 times its size.

It was also possible to determine through the EDS analysis (**Figure 13** and **Table 8**) that the charcoal obtained has the presence of charcoal, oxygen, and potassium. Although, part of these elements come from the coconut material, the oxygen present is the result of the carbonization and activation of the sample in the presence of air, and potassium is present in the endocarp, pulp, and water of the coconut [77].
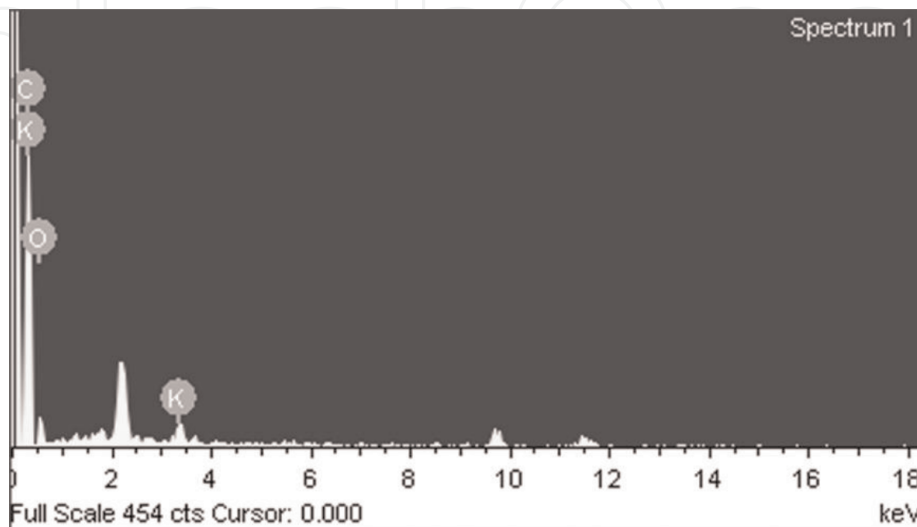
Figure 13.
Energy dispersive X-ray spectroscopy (EDS) of activated charcoal from coconut shell. Source: Energy dispersive X-ray spectroscopy, adapted to SEM.

Element	Mass %	Atomic %
C	75.58	81.03
O	22.98	18.50
K	1.44	0.47
Total	**100.00**	**100.00**

Table 8.
Composition of activated charcoal from coconut shell through energy dispersive X-ray spectroscopy (EDS).

6. Conclusions

This study revealed the potential of the coconut endocarp as a good precursor for the preparation of activated charcoal. The porous structure developed with a surface area, a total pore volume, and an average pore diameter, according to BET, of 526 m^2/g, 0.2341 cm^3/g, and 1.7784 nm, respectively, improves the adsorption process and indicates the presence of micropores. The equilibrium studies showed that the isotherm Langmuir model matches the adsorption data, meaning that the MO colorant adsorption forms a monolayer on the CACC. The adsorption capacity at equilibrium increased almost linearly when the concentration of MO solution increased from 80 to 400 mg/L. The equilibrium parameter R_L, obtained for the different initial concentrations of MO, indicates that the nature of adsorption is favorable. The thermodynamic parameters, that is, the negative values of Gibbs energy at the studied temperature, indicate, on one hand, the spontaneity of the adsorption process, reflecting the affinity of the charcoal obtained toward the anionic dyes, and on the other hand, that in the process are probably involved the physisorption and chemisorption. The SEM morphology analysis of CACC showed the presence of macropores and mesopores, which are characteristic of the activated charcoal. The results indicate that the activated charcoal obtained could be used as an alternative low-cost adsorbent in the MO removal from effluents in aqueous solutions.

Acknowledgements

Declaration of conflict of interests

The authors who appear in the article declare that there is no potential conflict of interests related to it.

Author details

Isabel Cristina Páez-Pumar Romer[†], Isabella Victoria Plazola Santana,
Rosa María Rodríguez Bengoechea and Miguel Manuel Pérez Hernández[*]
Universidad Metropolitana, Venezuela, Caracas

*Address all correspondence to: mperez@unimet.edu.ve

† These authors contributed equally.

IntechOpen

References

[1] Tsuboy MS, Angeli JPF, Mantovani MS, Knasmueller S, Umbuzeiro GA, Ribeiro LR. Genotoxic, mutagenic and cytotoxic effects of the commercial dye CI disperse blue 291 in the human hepatic cell line HepG2. Toxicology In Vitro. 2007; **21**(8):1650-1655. DOI: 10.1016/j.tiv.2007. 06.020

[2] Vinitnantharat S, Chartthe W, Pinisakul A. Toxicity of reactive red 141 and basic red 14 to algae and Waterfleas. Water Science and Technology. 2008; **58**(6):1193-1198. DOI: 10.2166/wst. 2008.476

[3] Anjaneyulu Y, Sreedhara-Chary N, Suman-Raj S. Decolourization of industrial effluents available methods and emerging technologies a review. Rev. Environ. Sci. Technol. 2005;**4**:245-273. DOI: 10.1007/s11157-005-1246-z

[4] Khelifi O, Nacef M, Affoune AM. Nickel (II) adsorption from aqueous solutions by physic-chemically modified sewage sludge. Iranian journal of chemistry and chemical engineering. 2018;**37**(1):73-87. DOI: 10.30492/ IJCCE.2018.29994

[5] Belaid KD, Kacha S. Etude cinétique et thermodynamique de l'adsorption d'un colorant basique sur la sciure de bois. Journal of Water Science. 2011, 2011;**24**(2):131-144. DOI: 10.7202/ 1006107ar

[6] Larakeb M, Youcef L, Achour S. Etude comparative de l'élimination du Zinc par adsorption sur la goethite et sur la bentonite de Maghnia. LARHYSS Journal. 2014;**19**(3):87-100. DOI: 10.7202/1006107ar

[7] Beijer E, Björlenius B, Shaik S, Lindberg RH, Brunström B, Brandt I. Removal of pharmaceuticals and unspecified contaminants in sewage treatment effluents by activated carbon filtration and ozonation: Evaluation using biomarker responses and chemical analysis. Chemosphere. 2017;**176**: 342-351. DOI: 10.1016/j.chemosphere. 2017.02.127

[8] Cazetta AL, Vargas AMM, Nogami EM, Kunita MH, Guilherme MR, Martins AC, et al. NaOH-activated carbon of high surface area produced from coconut shell: Kinetics and equilibrium studies from the methylene blue adsorption. Chemical Engineering Journal. 2011;**174**:117-125. DOI: 10.1016/j.cej.2011.08.058

[9] Arami M, Limaee NY, Mahmoodi NM, Tabrisi NS. Removal of dyes from colored textile wastewater by orange peel adsorbent: Equilibrium and kinetic studies. Journal of Colloid and Interface Science. 2005;**288**(2): 371-376. DOI: 10.1016/j.jcis.2005. 03.020

[10] Khelifi O, Nacef M, Affoune AM. Biosorption of nickel (II) ions from aqueous solutions by using chicken eggshells as low-cost biosorbent. Algerian Journal of Environmental Science and Technology. 2016;**2**(1): 12-16. ISSN: 2437-1114

[11] Hazourli S, Ziati M, Hazourli A, Cherifi M. Valorisation d'un résidu naturel ligno-cellulosique en charbon actif - exemple des noyaux de dattes. In: Revue des énergies renouvelables. Algeria: ICRESD-07 Tlemcen; 2007. pp. 187-192

[12] Pekkuz H, Uzun İ, Güzel F. Kinetics and thermodynamics of the adsorption of some dyestuffs from aqueous solution by poplar sawdust. Bioresource

Technology. 2008;**99**(6):2009-2017. DOI: 10.1016/j.biortech.2007.03.014

[13] Li W, Yang K, Peng J, Zhang L, Guo S, Xia H. Effects of carbonization temperatures on characteristics of porosity in coconut shell chars and activated carbons derived from carbonized coconut shell chars. Industrial Crops and Products. 2008;**28**:190-198. DOI: 10.1016/j.indcrop.2008.02.012

[14] Mittal A, Malviya A, Kaur D, Mittal J, Kurup L. Studies on the adsorption kinetics and isotherms for the removal and recovery of methyl Orange from wastewaters using waste materials. Journal of Hazardous Materials. 2007;**148**(1–2):229-240. DOI: 10.1016/j.jhazmat.2007.02.028

[15] Sakr F, Sennaoui A, Elouardi M, Tamimi M, Assabbane A. Étude de l'adsorption du Bleu de Méthylène sur un biomatériau à base de Cactus. J. Mater. Environ. Sci. 2015;**6**(2):397-406. ISSN: 2028-2508 CODEN: JMESCN

[16] Ocampo-Perez R, Leyva-Ramos R, Mendoza-Barron J, Guerrero-Coronado RM. Adsorption rate of phenol from aqueous solution onto organobentonite: Surface diffusion and kinetic models. Journal of Colloid and Interface Science. 2011;**364**(1):195-204. DOI: 10.1016/j.jcis.2011.08.032

[17] Bernal V, Giraldo L, Moreno-Piraján JC. Adsorción de acetaminofén sobre carbones activados a diferente pH. Entalpía y entropía del proceso. Revista Colombiana de Quimica. 2018;**47**(2): 54-62. DOI: 10.15446/rev.colomb.quim.v47n2.68213

[18] Valentina B, Liliana G, Moreno Juan C. Caracterización textural y química de carbones activados preparados a partir de cuesco de palma africana (*Elaeis guineensis*) por activación química con CaCl2 y MgCl2. Revista

Colombiana de Quimica. 2018;**47**(2): 54-62. DOI: 10.15446/rev.colomb.quim.v47n2.68213

[19] Molina-Sabio M, Rodríguez-Reinoso F. Role of chemical activation in the development of carbon porosity. Colloid Surface. 2004;**241**:15-25. DOI: 10.1016/j.colsurfa.2004.04.007

[20] Boehm HP. Surface oxides on carbon and their analysis: A critical assessment. Carbon. 2002;**40**:145-149. DOI: 10.1016/S0008-6223(01)00165-8

[21] Guo J, Chong Lua A. Textural and chemical properties of adsorbent prepared from palm shell by phosphoric acid activation. Materials Chemistry and Physics. 2003;**80**:114-119. DOI: 10.1016/S0254-0584(02)00383-8

[22] Enio S, Eustaquio A, Rafael R, Fidel R. Características agronómicas y productivas de progenies de cocotero alto por enano, falcón-venezuela. Agronomía Tropical. 2003;**53**:17-32

[23] Giraldo L, Moreno-Piraján JC. Monolitos de Carbón Activado a partir de Cáscara de coco e impregnación con níquel y cobre. Revista Colombiana de Quimica. 2008;**37**(3):355-370. Recuperado de: http://www.scielo.org.co/pdf/rcq/v37n3/v37n3a09.pdf

[24] Mojica LC, Ramírez WM, Rincón NG, Blanco DA, et al. Síntesis de carbón activado proveniente de semillas de Eucalipto por activación física y química. Bogotá, Colombia: Universidad de Los Andes; 2012

[25] De la Hoz M, Sarmiento J. Carbón Activado: Alternativa para la Purificación de Gases de Combustión [Trabajo de Grado]. Venezuela: Universidad Metropolitana; 2018

[26] Academic. Naranja de metilo. 2010. Recuperado de: https://esacademic.com/dic.nsf/eswiki/565589

[27] Ramírez Llamas LA, Jacobo Azuara A, Martínez Rosales JM. Adsorción del naranja de metilo en solución acuosa sobre hidróxidos dobles laminares. Acta Universitaria. 2015;**25**(4):25-34. DOI: 10.15174/au.2015.778

[28] Ocholi OJ, Gimba CE, Ndukwe GI, Turoti M, Abechi SE, Edogbanya PRO. Effect of time on the adsorption of methylene blue, methyl Orange and indigo carmine onto activated carbon. IOSR Journal of Applied Chemistry (IOSR-JAC). 2016;**9**(9) Ver. I:55-62. DOI: 10.9790/5736-0909015562

[29] Zhe-Ming N, Sheng-Jie X, Li-Grng W, Fang-Fang X, Guo-Xiang P. Treatment of methyl orange by calcined layered double hydroxides in aqueous solution: Adsorption property and kinetic studies. Journal of Colloid and Interface Sciences. 2007;**316**(2):284-291. DOI: 10.1016/j.jcis.2007.07.045

[30] Kron DA, Holland BT, Wipson R, Maleke C, Stein A. Anion exchange properties of a mesoporous Aluminophosphate. Langmuir. 1999;**15**(23):8300-8308. DOI: 10.1021/la990553r

[31] Cisneros A, Fernandes E. Preparación de carbón activado a partir de residuos de torrefaccionado y carbonizado alcalino de biomasa vegetal (Equisetum Giganteum) [Tesis de Grado]. Universidad Metropolitana, Caracas, Venezuela; 2017

[32] Lopez-Ramon MV, Stoeckli F, Moreno-Castilla C, Carrasco-Marin F. On the characterization of acidic and basic surface sites on carbons by various techniques. Carbon. 1999;**37**:1215-1221

[33] Coasne B, Galarneau A, Gerardin C, Fajula F, Villemot F. Validity of the t-plot method to assess microporosity in hierarchical micro/mesoporous materials. Langmuir. 2014;**30**:13266-13274

[34] Páez-Pumar I, Plazola I. Obtención y evaluación de carbón activado a partir del endocarpio de coco (cocos nucifera) para la remoción de compuestos minerales en agua potable [Tesis de Grado]. Caracas, Venezuela: Universidad Metropolitana; 2019

[35] Subasioglu T, Bilkay IS. Determination of biosorption conditions of methyl Orange by Humicola fuscoatra. Journal of Scientific and Industrial Research. 2009;**68**(12): 1075-1077

[36] Tchuifon DR, Anagho SG, Njanja E, Ghogomu JN, Ndifor-angwafor NG, Kamgaing T. Equilibrium and kinetic modelling of methyl orange adsorption from aqueous solution using rice husk and egussi peeling. International Journal of Chemical Sciences. 2014;**12**(3): 741-761. ISSN: 0972-768X

[37] Saha TK, Bhoumik NC, Mahmooda SK, Hideki Ichikawa GA, Fukumori Y. Adsorption of methyl Orange onto chitosan from aqueous solution. J. Water Resource and Protection. 2010;**2**:898-906. DOI: 10.4236/jwarp.2010.210107

[38] Aboua KN, Soro DB, Diarra M, DIBI K, N'Guettia KR, Traore KS. Étude de l'adsorption du colorant orange de méthyle sur charbons actifs en milieu aqueux: influence de la concentration de l'agent chimique d'activation. Afrique Science. 2018; **14**(6):322-331

[39] Arenas IA, López JL. Espectrofotometría de absorción. Curso: Métodos de Laboratorio, Instituto de

Biotecnología, Universidad Nacional Autónoma de México; 2004. Recuperado de: http://www.ibt.unam.mx/computo/pdfs/met/espectrometria_de_absorcion.pdf

[40] Haris MR, Sathasivam K. The removal of methyl red from aqueous solution using banana pseudostem fibers. American Journal of Applied Sciences. 2009;**6**(9):1690-1700

[41] Gamarra CG, La Rosa-Toro A. Decoloración del anarajado de metilo empleando el sistema fenton. Rev Soc Quím Perú. 2014;**80**(1):24-34. ISSN: 1810-634X

[42] Zhang PK, Wang L. Extended Langmuir equation for correlating multilayer adsorption equilibrium data. Separation and Purification Technology. 2010;**70**(3):367-371. DOI: 10.1016/j.seppur.2009.10.007

[43] Jeppu GP, Clement TP. A modified Langmuir-Freundlich isotherm model for simulating pH-dependent adsorption effects. Journal of Contaminant Hydrology. 2012;**129-130**:46-53. DOI: 10.1016/j.jconhyd.2011.12.001

[44] Naderi M. Chapter Fourteen - Surface Area: Brunauer–Emmett–Teller (BET). In: Tarleton S, et al. Progress in Filtration and Separation. UK: Academic Press; 2015, pp. 585-608, ISBN 9780123847461, DOI: 10.1016/B978-0-12-384746-1.00014-8

[45] Shaw D. Química de superficie y coloides. Madrid, España: Ediciones, Alhambra, S.A; 1977

[46] Lazo JC, Navarro A, Sun-Kou MR, Llanos BP. Síntesis y caracterización de arcillas organofílicas y su aplicación como adsorbentes del fenol. Rev. Soc. Quim. Perú. 2008;**74**(1):3-19. Disponible

en: http://www.redalyc.org/articulo.oa?id=371937608002

[47] Ahmad M, Rajapaksha AU, Lim JE, Zhang M, Bolan N, Mohan D, et al. Biochar as a sorbent for contaminant management in soil and water. Chemosphere. 2014;**99**:19-33. DOI: 10.1016/j.chemosphere.2013.10.071

[48] Ramírez A, Anyi P, et al. Preparación de carbón activado a partir de residuos de palma de aceite y su aplicación para la remoción de colorantes. Revista Colombiana de Quimica. 2017;**46**(1):33-41. DOI: 10.15446/rev.colomb.quim.v46n1.62851

[49] Castellan G. Fisicoquimica. Segunda edición. Editorial Pearson. Míxico: Addison Wesley Iberoamericana, S.A; 1987

[50] Zhou X, Zhou X. The unit problem in the thermodynamic calculation of adsorption using the Langmuir equation. Chemical Engineering Communications. 2014;**201**(11):1459-1467. DOI: 10.1080/00986445.2013.818541

[51] Liu Y. Is the free energy change of adsorption correctly calculated? Journal of Chemical & Engineering Data. 2009;**54**(7):1981-1985. DOI: 10.1021/je800661q

[52] Sarmiento C, Sánchez J, García C, Rincón Y, Benítez A, Ramírez J. Preparación de carbón activado mediante la activación química de carbón mineral [Trabajo de grado]. Maracaibo, Venezuela: Universidad del Zulia; 2004

[53] Carriazo JG, Saavedra MJ, Molina MF. Propiedades adsortivas de un carbón activado y determinación de la ecuación de Langmuir empleando materiales de bajo costo. Educ. quím. 2010;**21**(3):224-229. © Universidad

Nacional Autónoma de México, ISSN 0187-893-X Publicado en línea el 3 de mayo de 2010, ISSNE 1870-8404

[54] Inamuddin AMA, Mohammad A. Organic Pollutants in Wastewater I: Methods of Analysis, Removal and Treatment. Vol. 29. India. USA. Capítulo 4: Publicado por Materials Research Forum LLC; 2018. pp. 101-103. ISBN 194529163X, 9781945291630

[55] Wenzhong S, Zhijie L, Yihong L. Surface chemical functional groups modification of porous carbon. Recent Patents on Chemical Engineering. 2008; **1**:27-40. DOI: 10.2174/2211334710801010027

[56] Figueiredo JL, Pereira MFR, Freitas MMA, Orfao JJM. Modification of the surface chemistry of activated carbons. Carbon. 1999;**37**(9):1379-1389. DOI: 10.1016/S0008-6223(98)00333-9

[57] Van Der Kamp KA, Qiang D, Aburub A, Wurster DE. Modified Langmuir-like model for modeling the adsorption from aqueous solutions by activated carbons. Langmuir. 2005; **21**(1):217-224. DOI: 10.1021/la040093o

[58] Bernal V, Liliana Giraldo L, Moreno-Piraján JC. Adsorción de acetaminofén sobre carbones activados a diferente pH. Entalpía y entropía del proceso. Revista Colombiana de Quimica. 2018;**47**(2): 54-62. DOI: 10.15446/rev.colomb.quim. v47n2.68213

[59] De Boer JH, Custers JFH. Adsorption by van der Waals forces and surface structure. Physica. 1937;**4**(10): 1017-1024. DOI: 10.1016/S0031-8914 (37)80199-8

[60] Kong L, Adidharma H. A new adsorption model based on generalized van der Waals partition function for the description of all types of adsorption

isotherms. Chemical Engineering Journa l. 2019;**375**:122112. DOI: 10.1016/j.cej. 2019.122112

[61] Fulazzaky MA. Study of the dispersion and specific interactions affected by chemical functions of the granular activated carbons. Environme ntal Nanotechnology, Monitoring & Management. 2019;**12**:100230. DOI: 10.1016/j.enmm.2019.100230

[62] Knözinger E, Schüth F, Weitkamp J. Handbook of heterogeneous catalysis. 2., completely revised and enlarged edition. Vol. 1–8. Angewandte Chemie International Edition. 2009;**48**(19): 3390-3391. DOI: 10.1002/anie.200901598

[63] Yusoff S, Kamari A, Putra W, Ishak C, Mohamed A, Hashim N, et al. Removal of Cu (II), Pb (II) and Zn (II) ions from aqueous solutions using selected agricultural wastes: Adsorption and characterisation studies. Journal of Environmental Protection. 2014;**5**: 289-300. DOI: 10.4236/jep.2014.54032

[64] Castro JB, Bonelli PR, Cerrella EG, Cukierman AL. Phosphoric acid activation of agricultural residues and bagasse from sugar cane: Influence of the experimental conditions on adsorption characteristics of activated carbons. Industrial and Engineering Chemistry Research. 2000;**39**(11):4166-4172. DOI: 10.1021/ie0002677

[65] Barrett EP, Joyner LG, Halenda PP. The determination of pore volume and area distributions in porous substances. I. Computations from nitrogen isotherms. Journal of the American Chemical Society. 1951;**73**:373-380. DOI: 10.1021/ja01145a126

[66] Özcan M, Solmaz R, Kardaş Dehri I. 2008 adsorption properties of

barbiturates as green corrosion inhibitors on mild steel in phosphoric acid colloids and surfaces. Physicochem. Eng. Aspects. 2008;**325**:57-63. DOI: 10.1016/j.colsurfa.2008.04.031

[67] Milonjic SK. A consideration of the correct calculation of thermodynamic parameters of adsorption. Journal of the Serbian Chemical Society. 2007;**72**(12):1363-1367. DOI: 10.2298/JSC0712363M

[68] Saxena A, Prasad D, Haldhar R, Singh G, Kumar A. Use of Sida cordifolia extract as green corrosion inhibitor for mild steel in 0.5M H2SO4. Journal of Environmental Chemical Engineering. 2018;**6**(1):694-700. DOI: 10.1016/j.jece.2017.12.064

[69] Soldatkina L, Zavrichko M. Equilibrium, kinetic, and thermodynamic studies of anionic dyes adsorption on corn stalks modified by Cetylpyridinium bromide. Colloids and Interfaces. 2018, 2018;**3**(1):4. DOI: 10.3390/colloids3010004

[70] Huang ZN, Wang X, Yang DS. Adsorption of Cr (VI) in wastewater using magnetic multi-wall carbon nanotubes. Water Science and Engineering. 2015;**8**(3):226-232. DOI: 10.1016/j.wse.2015.01.009

[71] Budi E, Nasbey H, Yuniarti BDP, Nurmayatri Y, Fahdiana J, Budi AS. Pore structure of the activated coconut shell charcoal carbon. In: AIP Conference Proceedings 1617. Indonesia: AIP Publishing LLC; 2014. pp. 130-133. DOI: 10.1063/ 1.4897121

[72] Wei L, Yang K, Peng J, Libo Z, Sheughui G, Hongying X. Effects of carbonization temperatures on characteristics of porosity in coconut Shell chars and activated carbons derived from carbonized coconut Shell chars. Industrial Crops and Products.

2008;**28**(2):190-198. DOI: 10.1016/j.indcrop.2008.02.012

[73] Xinying W, Danxi L, Wei L, others. Optimization of mesoporous activated carbon from coconut shells by chemical activation with phosphoric acid. BioResources. 2013;**8**(4):6184-6195. DOI: 10.15376/biores.8.4.6184-6195

[74] Katesa J, Junpiromand S, Tangsathitkulchai C. Effects of carbonization temperature on porous properties of coconut Shell based activated carbon. Journal of Science and Technology. 2013;**20**(4):269-278. Corpus ID: 98597508

[75] Achaw O-W. A Study of the Porosity of Activated Carbons Using the Scanning Electron Microscope, Scanning Electron Microscopy, Viacheslav Kazmiruk. Rijeka: IntechOpen; 2012. DOI: 10.5772/ 36337. Available from: https://www.intechopen.com/chapters/30949

[76] Ab. Jabal SN, Seok YB, Wee FH. Carbon composition, surface porosities and dielectric properties of coconut Shell powder and coconut Shell activated carbon composites. ARPN Journal of Engineering and Applied Sciences. 2016; **11**(6):3832-3837. Corpus ID: 136667440. ISSN 1819-6608

[77] Coconut water is it, F.A.O. http://www.fao.org/News/2000/000902-e.htm. Última visita, 15/03/2020; 14:30 horas